

Application of thermovision method to welding thermal cycle analysis

J. Nowacki ^{a,*}, A. Wypych ^b

^a Institute of Materials Science and Engineering, West Pomeranian University of Technology, Al. Piastów 19, 70-310 Szczecin, Poland

^b Institute of Materials Science and Engineering, Poznan University of Technology, pl. M. Skłodowskiej-Curie 5, 60-965 Poznań, Poland

* Corresponding author: E-mail address: jnowacki@zut.edu.pl

Received 20.01.2010; published in revised form 01.06.2010

Methodology of research

ABSTRACT

Purpose: of this paper is to determine the possibility of of thermovision method application in the thermal cycle of Inconel 625 on 13CrMo4-5 steel pad welding thermal cycle analysis.

Design/methodology/approach: Single- and multibead pad welding of steel 13CrMo4-5 by superalloy Inconel 625 has been carried out by means of GMA method in inert gas backing shielding, in horizontal position and 620 J/mm and 2100 J/mm heat input level. Quantitative data concerning infrared radiation emission as a basis for evaluation of thermal history of the applied object in order to assist interpretation changes occurring in padding welds and heat-affected have been obtained on the grounds of infrared radiation measurement by means of Flir Systems ThermaCAM SC2000 PAL infrared camera.

Findings: As a result of the performed inspection, temperature distribution in the weld made by heat input energy $E = 2100$ J/mm; of cooling, both cooling curves of padding welds and HAZ during single- and multi sequence pad welding have been determined and also single bead self-cooling time and durability time during single bead pad welding.

Practical implications: The full suitability of thermovision analysis of thermal cycle of pad welding. Specified self-cooling times will become a base for inference about microstructural transforms in HAZ, whereas cooling rate settlement determines necessary conditions to maintaining required intersequence temperature for assumed heat level input of pad welding, padding weld temperature in self-cooling time function and particular.

Originality/value: The thermovision effect and thermal cycle of Inconel 625 on 13CrMo4 -5 steel pad welding thermal cycle analysis has been no yet determined.

Keywords: Thermovision analysis; Superalloy padding welds; Welding thermal cycle; Temperature distribution in the weld

Reference to this paper should be given in the following way:

J. Nowacki, A. Wypych, Application of thermovision method to welding thermal cycle analysis, Journal of Achievements in Materials and Manufacturing Engineering 40/2 (2010) 131-137.

1. Introduction

Indirect investigations of temperature by infrared method depend on measurement infrared radiation emitted by applied object. The detection circuit of system transforms this radiation

into electric signal, which is the source of information about the temperature of the object.

To determine the fields and temperature values a thermometric diagram stored in the memory of the measuring device is used.

Apart from infrared radiation emitted by the applied object, the detective structure records also the radiation of the

environment reflected on the surface of the applied object, self-radiation emitted between the lens and the applied object as well as radiation of the internal parts of the camera which also reaches the radiation detector.

Distribution of spectral concentration of radiation power depends on measurement conditions, which consist of dustiness, humidity, pressure and emission of objects. Taking into consideration all the factors that have an influence upon measurement values, infrared camera requires calibration on true object.

Obtaining a reliable result is possible after marking a calibration curve. Radiation methods used for temperature measurements require introduction of emissivity coefficient to the system, which describes radiation properties dependent on:

- tested material,
- surface layer condition,
- radiation angle,
- radiation wavelength,
- surface shape of applied object,
- temperature of applied object (Fig. 1).

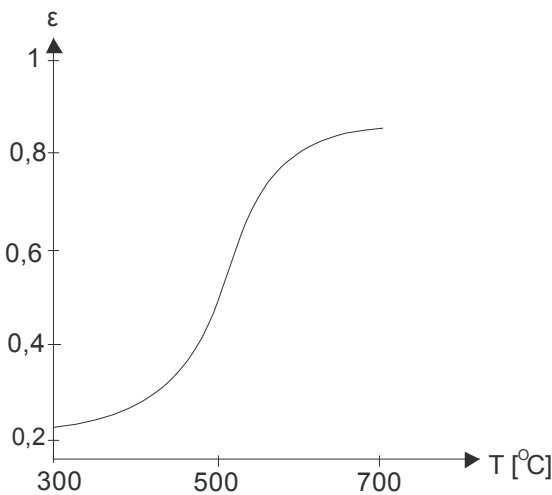


Fig. 1. Transformation of the total emissivity of 13CrMo4-5 steel in temperature function [1]

Parameters describing emission properties of materials are as following:

- normal emissivity,
- directional emissivity,
- band emissivity,
- global emissivity,
- monochromatic emissivity.

Taking into consideration the complexity of temperature measurement device through infrared radiometric systems, the occurrence of an error is probable. Both slotted line and irregular calibration can be the reason for the error. Temperature measurement by means of radiation methods requires introducing efficient emissivity value to the system [1-5] (Eq. 1).

$$\varepsilon_{ef} = \frac{\int_{\lambda_1}^{\lambda_2} \varepsilon_R(\lambda) L(\lambda, T_{ob}) csk(\lambda) d\lambda}{\int_{\lambda_1}^{\lambda_2} L(\lambda, T_{ob}) csk(\lambda) d\lambda} \quad (1)$$

The heat flow in welding elements can be presented by a differential equation (Eq. 2)

$$\frac{\partial T}{\partial t} = \frac{\lambda}{c\rho} \left(\frac{\partial^2 T}{\partial x^2} + \frac{\partial^2 T}{\partial y^2} + \frac{\partial^2 T}{\partial z^2} \right) \quad (2)$$

λ – thermal conductivity

c – specific heat

ρ – material density

x, y, z - directions of heat diffusion

After boundary conditions acceptance, Eq. 2 abridges to:

$$T(t) = T_0 e^{-bt} \quad (3)$$

$T(t)$ – temperature at a given time of cooling,

T_0 – initial temperature,

t – time,

$$b = \frac{2\alpha}{c\rho g} \text{ – temperature coefficient of heat emission}$$

g – thickness of applied object.

Depending on time thermal field is a result of working out the differential equation as shown above (Eq. 3). After boundary conditions acceptance the formula is as following:

$$T = f(x, y, z, t) \quad (4)$$

T – testing point temperature

x, y, z, t , - space-time coordinates

To calculate thermal field one needs to make an assumption of analytical model according to heat flow area and heat source type. In the described experiment a massive body model has been applied, in which the heat flow is three-dimensional, undisturbed by external surface and moving point heat source in welding arc form.

Thermal change analysis in the applied object is a result of temperature gradient observation [1,2,6] Temperature evaluation of the applied object or its changes are possible as a consequence of application of diversified measurement methods like:

- non electrical (expansion, bimetallic, liquid and liquid crystal thermometers),
- ultrasonic,
- noise thermal,
- optical waveguide,
- thermo-electrical,

- thermal resistance,
- temperature-sensitive resistor,
- thermovision.

The widest measuring range of temperature (from -50°C to above 2000°C) is ensured by thermovision methods. The heat that is input to subsoil stuff in GMA welding process, besides padding welds creation, generates heating of the weld-affected zone to a temperature of microstructural transformation. These changes proceed on some surface that is characterized by this surface point distance from the heat source. Temperature of the points is a function of their distance from the welding arc as heat source and is dependent on welding arc thermal power [6,7]. Presently thermovision methods in materials processing have been strongly developed [8-14].

Microstructural range of changes occurs on the visible surface creating weld-affected zone. Multibead pad welding of steel 13CrMo4-5 by Inconel 625 superalloy, which is mainly used in cylinder head technology, requires maintaining interbead temperature ranging between 200 °C-250 °C. The process needs to be discontinued during pad welding to maintain required temperature.

Reheating or interrupting time settlement is a part of thermal cycle of welding analysis task.

2. Thermal cycle of pad welding steel 13CrMo4-5 by Inconel 625 superalloy investigation

Single- and multibead pad welding of steel 13CrMo4-5 by superalloy Inconel 625 has been carried out by means of GMA welding method (according to PN-EN ISO 4063) in inert gas backing shielding (Argon 4.6 MESSER), in horizontal position and 620 J/mm and 2100 J/mm heat input level (Table 1).

Table 1.

T_{8-5} time for HAZ of 13CrMo4-5 steel, t_{11-5} for padding weld of Inconel 625 superalloy and $t_{14-2,5}$ time of obtaining intersequence temperature $T = 250$ °C on breaking the arc

Welding heat input $Q, J/mm$	Time t_{8-5}, S	Time t_{11-5}, S	Time $t_{14-2,5}, S$
$Q = 620J/mm$	1.4	2.8	7.0
$Q = 2100J/mm$	4.7	10.2	55.0

Pad welding on $250 \times 150 \times 45$ overall dimensions samples were made by means of coiled electrode 1.2 mm diameter. Infrared spectrum during self-cooling has been recorded. Quantitative data concerning infrared radiation emission is a basis for evaluation of thermal history of the applied object. Measurements have been made in order to assist interpretation changes occurring in padding welds and heat-affected zone in a temperature under 1400°C.

Infrared spectrum has been obtained on the grounds of infrared radiation measurement by means of Flir Systems ThermoCAM SC2000 PAL infrared camera (Fig. 2). Camera has been positioned within the distance of 1 meter from infrared range

emitter sample. Measurement has been taken in 25°C temperature, with no air movements and 30% humidity. Accuracy of measurement amount to 2% of indicated measurement value. ThermoCAM Reporter software has been used to work out the documentation. Emissivity coefficient value has been specified on the grounds of scientific literature.

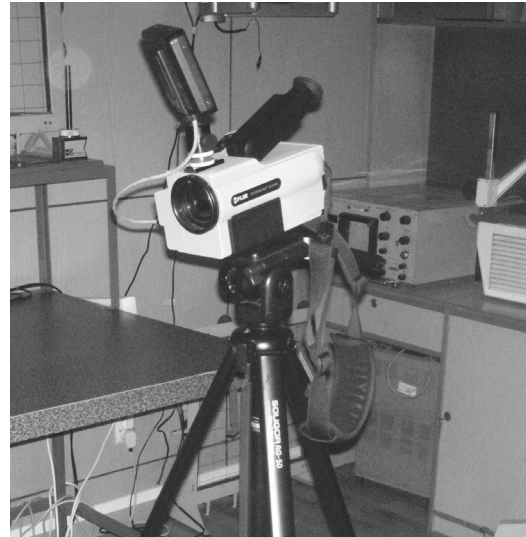


Fig. 2. ThermoCAM SC2000 PAL Flir Systems thermovision camera used in the experiment

Taking into consideration the steel base of the surface condition – milling, oxidation, heating to high temperature, covering with deposit weld layer and environment of the measurement, emissivity coefficient has been determined $\epsilon_{st} = 0.85$.

Oxide coating superalloy emissivity coefficient is $\epsilon_{In} = 0.86$.

Pad welding and base radiation measurement has been made according to flow chart (Figs. 3, 4). In the result of heat source forming welding arc action, heat flow in base material is in progress according to YZ uniplanar isothermal line. Single extreme isotherm points lying along dashed line on XY plane have been used to infrared radiation measurement emitted by XY plane of the applied object. The highest radiation power points provide information about the maximal base material temperature.

Padding welds radiation measurement on YZ plane has been taken by measuring radiation power of a very small area in the vicinity of origin of coordinates location (Fig. 4). In the consequence of measurements both cooling curves of padding welds and HAZ during single- and multi - sequence pad welding have been determined and also single bead self-cooling time and durability time during single bead pad welding (Fig. 5 - Fig. 14).

For HAZ base material t_{8-5} time has been determined. For padding weld for the sake of critical range of microstructural changes, temperature in Inconel 625 superalloy, t_{11-5} has been evaluated (Table 1, Fig. 15). Native and addition material temperatures value after pad welding were also estimates (Figs. 16-21).

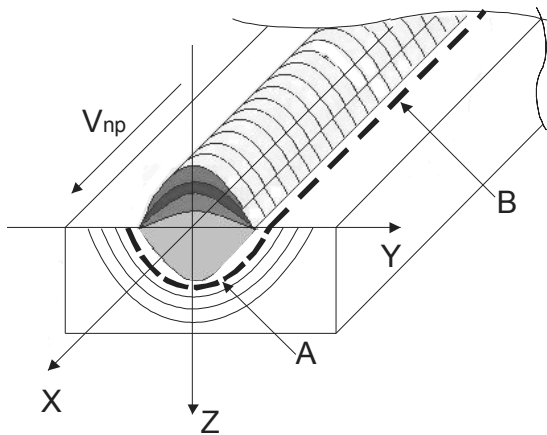


Fig. 3. Pad welding flow diagram; infrared radiation measurement along B broken line on XY plane; thermal field presented by means of A isothermal line on YZ plane formed simultaneously with moving the heat source in the direction of X-axis; V_{np} – pad welding direction; single sequence carried out according to the same flow diagram

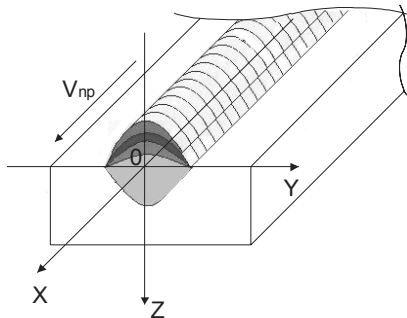


Fig. 4. Pad welding flow diagram; padding welds infrared radiation measurement on YZ plane; V_{np} – pad welding direction

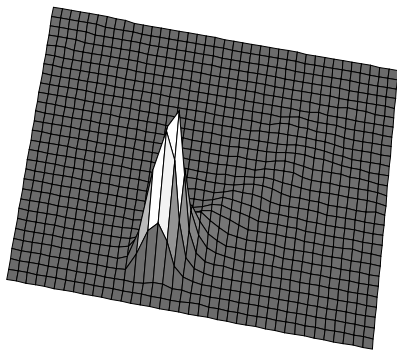


Fig. 5. Three-dimensional pictorial temperature distribution image after single - sequence pad welding with energy of $Q = 620$ J/mm

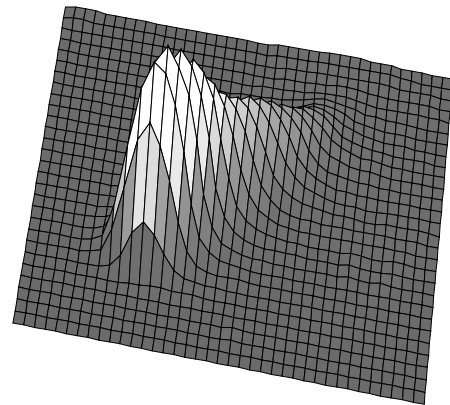


Fig. 6. Three-dimensional pictorial temperature distribution image after single sequence pad welding with energy of $Q = 2100$ J/mm

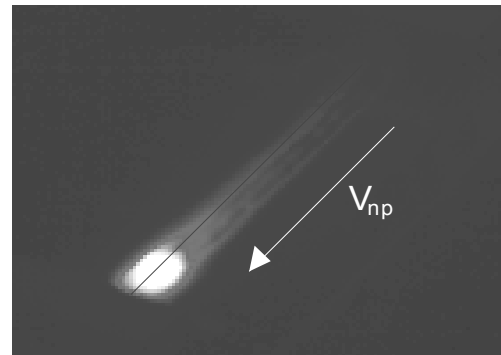


Fig. 7. Thermovision image of temperature distribution in the weld made by heat input energy $Q = 620$ J/mm; measured along V_{np} line (Fig. 3) after 1 second of cooling

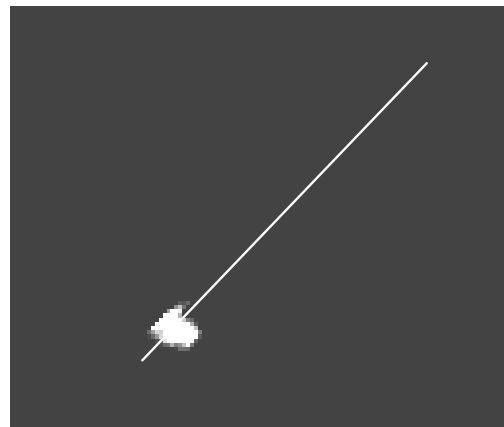


Fig. 8. Thermovision image of temperature distribution in the weld made by heat input energy $Q = 620$ J/mm; measured along V_{np} line (Fig. 3) after 7 second of cooling

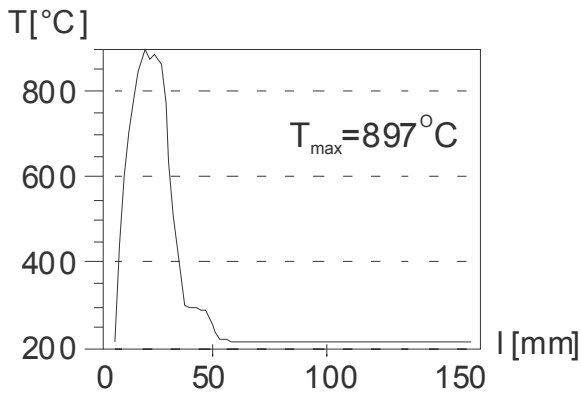


Fig. 9. Temperature distribution in the weld made by heat input energy $Q = 620$ J/mm; measured along V_{np} line (Fig. 3) after 1 second of cooling

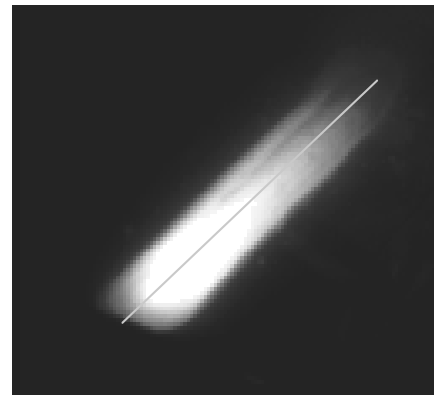


Fig. 12. Thermovision image of temperature distribution in the weld made by heat input energy $Q = 2100$ J/mm; measured along V_{np} line (Fig. 3) after 7 second of cooling

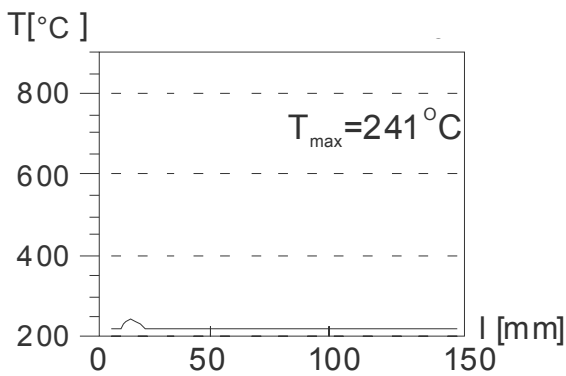


Fig. 10. Temperature distribution in the weld made by heat input energy $Q = 620$ J/mm; measured along V_{np} line (Fig. 3) after 7 second of cooling

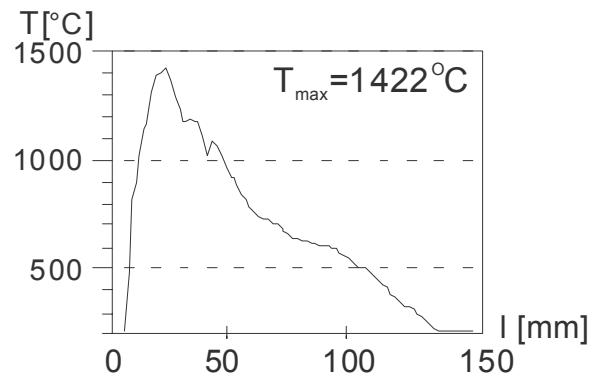


Fig. 13. Temperature distribution in the weld made by heat input energy $Q = 2100$ J/mm; measured along V_{np} line (Fig. 3) after 1 second of cooling

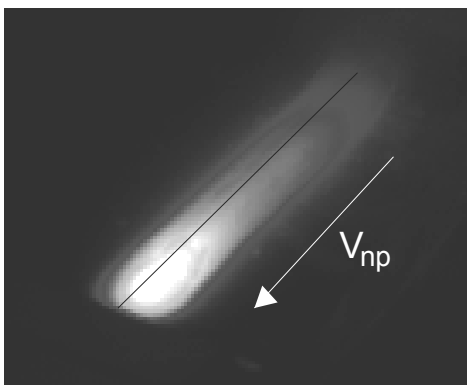


Fig. 11. Thermovision image of temperature distribution in the weld made by heat input energy $Q = 2100$ J/mm; measured along V_{np} (Fig. 3) line after 1 second of cooling

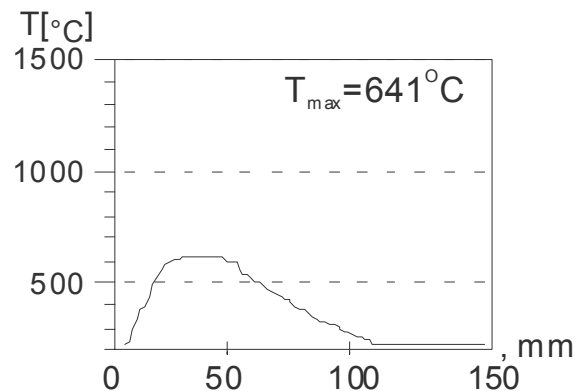


Fig. 14. Temperature distribution in the weld made by heat input energy $Q = 2100$ J/mm; measured along V_{np} line (Fig. 3) after 7 second of cooling

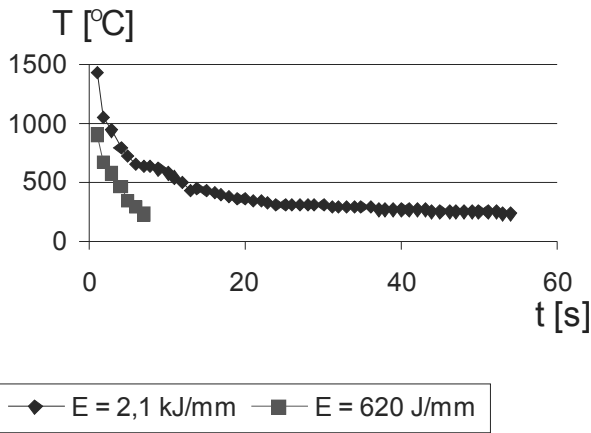


Fig. 15. Padding weld temperature in self-cooling time function; single sequence pad welding by Q = 620 J/mm and Q = 2100 J/mm heat input energy

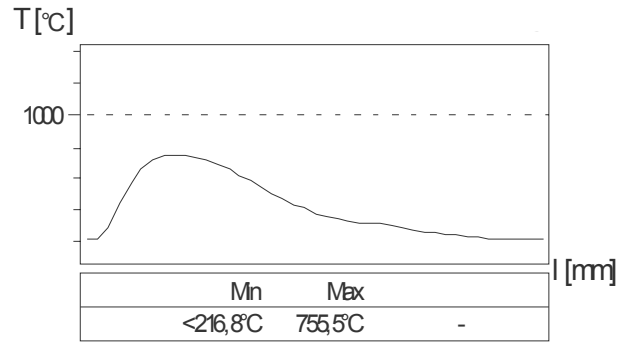


Fig. 18. Parent material temperature value, measured along B line (Fig. 3) after pad welding by Q = 2100 J/mm energy, first bad

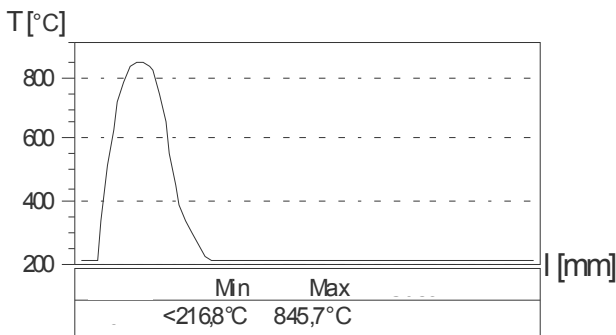


Fig. 16. Native material temperature value, measured along B line (Fig. 3) after pad welding by Q = 620J/mm energy, first bad

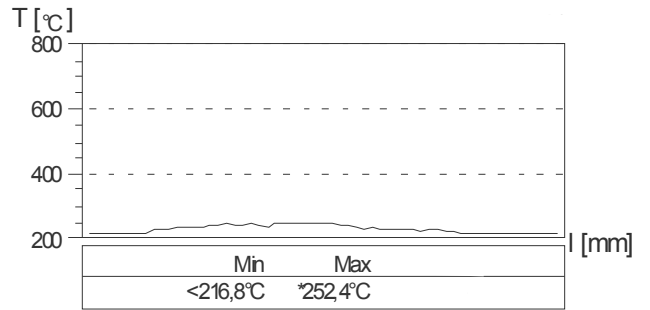


Fig. 19. Parent material temperature value, measured along B line (Fig. 3) after pad welding by Q = 2100 J/mm energy, b) last bad

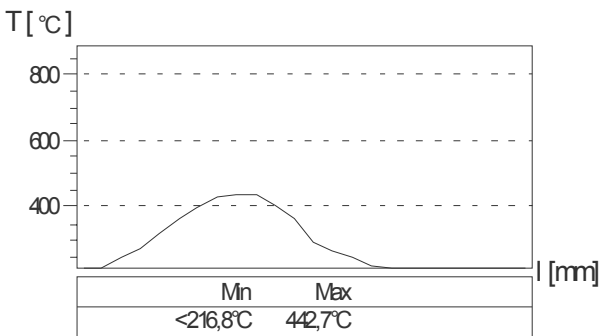


Fig. 17. Native material temperature value, measured along B line (Fig. 3) after pad welding by Q = 620J/mm energy last bad

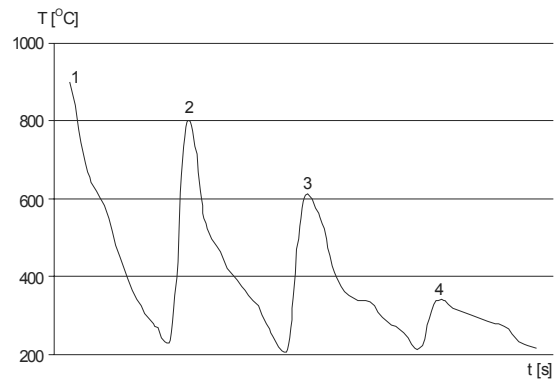


Fig. 20. Temperature transform curve of Inconel 625 superalloy sealing run during multisequence pad welding by Q = 620 J/mm heat input energy after making the following sequences 1 to 4 – numbers of the following sequences

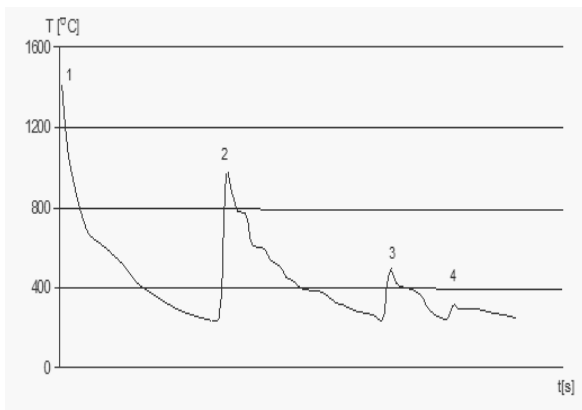


Fig. 21. Temperature transform curve of Inconel 625 superalloy sealing run during multisequence pad welding by $Q = 2100 \text{ J/mm}$ heat input energy; 1 to 4 – numbers of the following sequences

3. Conclusions

The conducted investigation of Inconel 625 superalloy on 13CrMo4-5 steel pad welding thermal cycle has shown a full suitability of thermovision engineering in thermal cycle of pad welding analysis.

Specified self-cooling times will become a base for inference about microstructural changes in HAZ, whereas cooling rate settlement determines necessary conditions to maintaining required intersequence temperature for assumed heat level input of pad welding.

The applied method can be characterized by great versatility and it enables estimation of linear, flat and spatial temperature distribution in the following welding sequence; it also enables intersequence temperature control of $t_{8,5}$ time or other characteristic times regarding temperature range of phase changes and separation processes in non-ferrous alloys. Moreover, it enables estimation of breaks from welding - necessary in maintaining assumed intersequence temperature as well as versatile analysis of padding weld thermal course (history) in a very wide range of temperatures. Restrictions to application of thermovision method to thermal cycle analysis can be a low availability of thermovision systems due to high prices of this plant.

Acknowledgements

The authors wish to thank dr inż. Leszek Rózański and mgr inż. Marian Stroiński from Mechanical Technology Institute, Machine Building and Management Department of Poznan University of Technology for help in monitoring thermovision tests of pad welding processes.

The authors are grateful to the Ministry of Science and Higher Education for financing the research project MNiSW No. N N507 356635 within the scope of which possibility of this paper publication was created.

References

- [1] N.K. Ravala, H. Fan, H.C. Wikle III, B.A. Chin, Modeling and sensing for penetration control of the saw process in the presence of welding perturbations, Proceedings of the American Society of Mechanical Engineers Heat Transfer/Fluids Engineering Summer Conference, Charlotte, North Carolina, 2004, 945-952.
- [2] H. Fan, N.K. Ravala, H.C. Wikle III, B.A. Chin, Low-cost infrared sensing system for monitoring the welding process in the presence of plate inclination angle, Journal of Materials Processing Technology 140/1-3 (2003) 668-675.
- [3] D. Dehelean, V. Safta, R. Cojocaru, T. Hälker, C. Ciucă, Monitoring the quality of friction stir welded joints by infrared thermography, Welding in the World 52 (2008) 621-626.
- [4] A. Cobo, J. Mirapeix, O.M. Conde, P.B. García-Allende, F.J. Madruga, J.M. López-Higuera, Arc welding process control based on back face thermography: Application to the manufacturing of nuclear steam generators, Proceedings of the SPIE 6541 (2007).
- [5] Z. Zheng, P. Shan, S. Hu, X. Wei, J. Yang, Numerical simulation of gas metal arc welding temperature field, China Welding 15/4 (2006) 55-58 (English Edition).
- [6] F. Bardin, S. Morgan, S. Williams, R. McBride, A.J. Moore, J.D.C. Jones, Process control of laser conduction welding by thermal imaging measurement with a color camera, Applied Optics 44/32 (2005) 6841-6848.
- [7] J. Nowacki, A. Wypych, Evaluation of the inconel 625 superalloy on 13CrMo4-5 steel pad welding thermal cycle by thermovision method, Welding Review 12 (2007) 3-7.
- [8] Z. Rdzawski, B. Krupińska, M. Muszyfaga, Thermovision systems used to improve a technological process for hot-rolled copper and brass strips, Journal of Achievements in Materials and Manufacturing Engineering 36/2 (2009) 115-125.
- [9] G. Rudowski, Thermovision and its application, WKiN, Warsaw, 1978.
- [10] G.M. Carlomagno, Quantitative applications of infrared thermography in fluid mechanics, Proceedings of the Conference "Thermography and Infrared Thermometry", Warszawa, 1996, 55-76.
- [11] Z. Bogdanowicz, W. Napadlek, M. Prejskorn, Studies of stresses and their slow cooling for casting process using thermovision, Bulletin of the Military University of Technology 01 (2003) 125-136.
- [12] Z. Rdzawski, W. Pala, The application examples of thermovision examinations in the non-ferrous metal industry, Proceedings of the 3rd Conference TTP'96, Warszawa, 1996, 177-182.
- [13] G. Wróbel, G. Muzia, Z.M. Rdzawski, M. Rojek, J. Stabik, Thermographic diagnosis of fatigue degradation of epoxy glass composites, Journal of Achievements in Materials and Manufacturing Engineering 24/1 (2007) 131-136.
- [14] G. Muzia, Z.M. Rdzawski, M. Rojek, J. Stabik, G. Wróbel, Thermographic diagnostic of fatigue degradation of epoxy glass composites, Journal of Achievements in Materials and Manufacturing Engineering 24/2 (2007) 123-126.